Chalcogenide Letters Vol. 15, No. 1, January 2018, p. 35 - 43

PHOTOINDUCED MASS TRANSPORT IN Ge-Se AMORPHOUS FILMS

M. REINFELDE[a], M. MITKOVA[b], T. NICHOL[b], Z.G. IVANOVA[c], J. TETERIS[a*]
[a]*Institute of Solid State Physics, University of Latvia, Riga, Latvia*
[b]*Department of Electrical and Computer Engineering, Boise State University, USA*
[c]*Institute of Solid State Physics, Bulgarian Academy of Sciences, Sofia, Bulgaria*

The photoinduced surface relief grating (SRG) formation in chalcogenide Ge_xSe_{1-x} ($0 \leq x < 0.4$) thin films is studied. An increase of SRG formation efficiency and photoinduced birefringence is observed for the films with an excess of selenium content ($x < 0.33$). In the process of SRG formation the photoinduced displacement of film material takes place from *s*- to *p*- polarization direction state in interference pattern of light. Energy Dispersive Spectroscopy (EDS) data show compositional changes between SRG *top* and *bottom* positions.

(Received September 30, 2017; Accepted January 11, 2018)

Keywords: Holographic recording, chalcogenide films, photoinduced mass transport

1. Introduction

Photoinduced structural changes in soft materials play the key role in advanced technologies: chalcogenide thin films are used as storage media of information (audio/videodisks); organic and inorganic photoresists and related materials necessary to produce advanced electronics hardware. Photoinduced alignment of molecules in azo-containing polymers causes an appearance of optical birefringence – the basic condition for polarization holographic recording materials. Recently it has been shown that under influence of linear polarized light a lateral transfer of matter is possible allowing to realize "one step" surface patterning.

Already in 1976 Chomat *et al* [1] showed that a thin film of an amorphous As_2Se_3 subjected to an intensity modulated red light interference pattern was significantly altered: a relief hologram was formed on the surface of the film. Almost twenty years later a similar phenomenon for thin layers of azobenzene-containing polymers was observed by Rochon *et al* [2] and Kim *et al* [3]. A flat film can reach a corrugation whose amplitude may be up to fifty per cent of the initial thickness. This suggests that the material moieties are put in light-induced lateral transfer regarding the propagation direction of exciting light. The most commonly used method to induce mass motion is holographic recording with which a sinusoidal modulated intensity pattern can be obtained at the submicron scale. The surface relief structures can be formed also by a focused light spot [4] and illumination performed via a metal microgrid placed on the sample [5]. Recently, the surface relief grating recording only by one laser beam with lateral modulated polarisation directions was demonstrated [6]. The surface patterns can be erased by homogeneous illumination or heating above glass transition temperature of recording media. The surface relief grating direct formation by two coherent laser beam interference has been observed in different disordered materials: in amorphous inorganic (As-S, As-Se) chalcogenides [7], Sb-P-O oxide-containing glass [8] and many organic azobenzene-containing polymers [2,3,9] and organic low-molecular glasses [10]). The efficiency of SRG formation on the azobenzene containing polymer and chalcogenide semiconductor films strongly depends on the polarization state of the recording beams [11]. The largest surface relief (SR) modulation can be obtained under $+45^0$:-45^0 (linearly orthogonal polarization with a direction 45^0 regarding the plane of recording beams) and RCP:LCP (right and

*Corresponding author: teteris@latnet.lv

left circular polarization of beams) recording conditions. This indicates that the existence of both light intensity and resultant electric field variations are essential to the formation of SRG on amorphous chalcogenide films.

The phenomenon of photoinduced mass transport has mainly studied in chalcogenide materials from As-S(Se) systems. Less data are available for the Ge-S and Ge-Se systems. Recently the amorphous Ge-Se films have received much attention as a potentional material for the fabrication of resistance random access memory (ReRAM) based on the electrochemical control of diffused metal ions (Ag) in chalcogenide thin films [12,13]. Light and electron beam induced surface patterning in Ge-Se system amorphous films were studied by Csarnovics et. al. [14,15].

The main goal of this paper is to explore the surface relief grating formation efficiency in amorphous Ge_xSe_{1-x} ($0 \le x < 0.4$) films, its dependence on recording laser wavelength as well as to establish the relationship between the surface relief formation efficiency and photoinduced anisotropy in the films.

2. Experimental

Ge_xSe_{1-x} ($0 \le x < 0.4$) films were prepared by thermal flash-deposition in vacuum on glass or Si substrates. The film thickness was about 1 μm. The schemes for holographic recording and

birefringence measurements are shown in Fig. 1 a, b, respectively. The lasers with wavelengths of 491 nm, 532 nm, 561 nm and 594 nm were used for holographic recording of gratings. Intensity of each recording beam was about 0.3 W/cm^2. Diffraction efficiency in transmission mode was measured by 645 nm laser ((L2) but in reflection mode by recording laser diffracted reflection light (beam P_R). The phase relationship between the exciting light field and the resulting surface deformation (see Fig. 7) was measured by method described in [16]. The surface of holographic gratings was investigated by atomic force microscope. Experimental set-up for photoinduced birefringence measurements is described in [17]. Birefringence was induced and measured at 532 nm and 635 nm wavelengths.

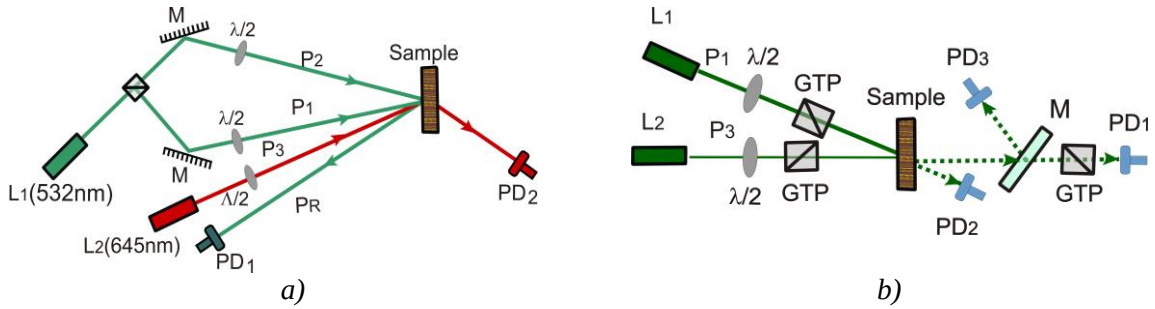

Fig.1 Experimental setup for holographic recording (a) and photoinduced birefringence measurements (b): L1, L2- lasers, P1,P2 – exitation beams, P3 – probing and P_R - refracted light beams, λ/2(λ /4) half wave plates, GTP – Glan-Tylor prism, PD – photodiodes.

A value of birefringence was evaluated according to formula:

$$\Delta n = \frac{\lambda}{\pi d} \arcsin\left(\sqrt{\frac{I}{I_0}}\right) \tag{1}$$

where I is the probe beam intensity passing through crossed polarizer and analyzer, I_0 – probe beam intensity passing through parallel polarizers (with transmittance changes taken into account), λ - probe wavelength and d is the thickness of the studied film.

3. Results and discussion

The samples of Ge_xSe_{1-x} thin films deposited on Si and glass substrates were used to test the dependence on composition ($0 \le x \le 0.4$), recording laser wavelength (491 nm, 561 nm and 594 nm) and grating period (1 μm and 5.7 μm) for SRG formation efficiency. Holographic recording was performed with linearly polarized beams with $\pm 45^0$ configuration of polarization direction. Recording process was controled by diffraction efficiency in reflection mode (light beam P_R) measured by photodiode PD_1 (see Fig.1a). All SRG recording experiments were completed at recording exposure dose 10.8 kJ/cm^2. Following SRG recording, each sample was measured by Atomic Force Spectroscopy (AFM) to analyze the surface topography. From the obtained data shown in Fig. 2, which displays the grating heights of multiple compositions of Ge_xSe_{1-x} system, wavelengths used for recording, and grating periods, it can be seen that this system is most sensitive to the 594 nm laser and for large period gratings. The compositional dependence shows an increase of SRG formation efficiency for the Ge_xSe_{1-x} films with an excess of selenium content ($x<1/3$). The maximum depth (Δh=290 nm) of gratings was obtained for Se and $Ge_{10}Se_{90}$ films. The SRG formation efficiency in $GeSe_2$ and in the germanium-rich range ($x>1/3$) is insignificant, but for the selenium-rich ($x<1/3$) films continuous increse of Δh is observed. These results are in agreement with the previous reports [14,15]. The reduction in efficiency seen for Se films in the case of recording using 491nm and 561 nm lasers is probably a result of α-Se crystallization due to strong light absorption.

According to [18] the short wavelength absorption edge in Ge_xSe_{1-x} films takes a maximum value at around $x=1/3$ (for stoichiometric $GeSe_2$ compound). For selenium-rich ($0 \le x < 1/3$) amorphous films a significant reduction of mean atomic bonding energy, glass transition temperature and optical bandgap has been observed by an increase of selenium content in the films. Twofold coordinated selenium atoms cause an increase of atomic mobility thus promoting the photoinduced mass displacement process.

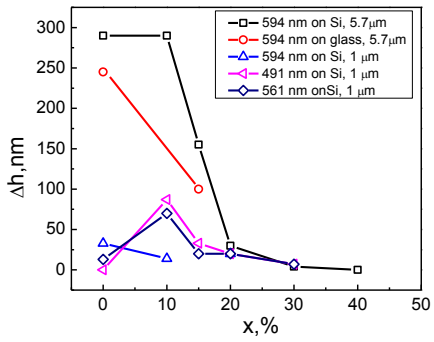

Fig.2 The SRG profile height on Ge_xSe_{100-x} films at holographic recording by 491 nm, 561 nm and 594 nm laser beams with $+45^0$ and -45^0 polarization, intensity of recording beams $I_1=I_2=0.3$ W/cm^2, grating period 1 and 5.7 μm.

Fig. 3 presents the dependence of diffraction efficiency (*DE*) and SRG depth (Δh) on composition of Ge_xSe_{100-x} films at holographic recording by 532 nm laser beams with right circular polarization (RCP) and left circular polarization (LCP) configuration. *DE* was registered during holographic recording process by measuring the diffracted light (beam P_R) of recording beams in reflection mode by photodiode PD_1 (see Fig. 1a). A substantial increase of *DE* and Δh is observed in the films with $x<33$ when the films possess an excess of Se concentration. It is seen that the measured *DE* of SRG is in a good correlation with the grating depth (Δh). It allows a checking of grating depth during holographic recording process that is very important for practical fabrication of the gratings with definite relief depth. As example, the grating depth $\Delta h>300$ nm can be obtained on the $Ge_{25}Se_{75}$ films (see Fig. 4). It is known that the optimum depth of SRG for

holographic display in visible spectral region is a half of light wavelength (λ/2). Diffraction efficiency measurements by recording beam light in reflection mode give an information only about surface relief changes because the light phase shift is caused by surface relief.

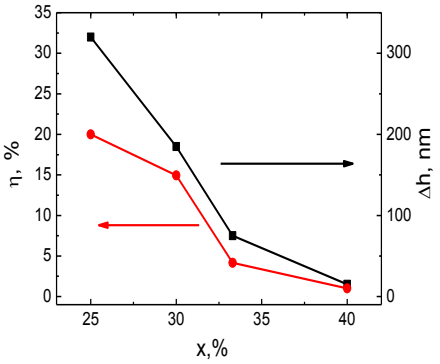

Fig. 3. Diffraction efficiecy and the profile depth (Δh) dependence of Ge_xSe_{100-x} films by LCP-RCP polarisation recording with 532 nm laser, intensity $I_1=I_2=0.3W/cm^2$, grating period $\Lambda=1$ μm.

To get information about holographic recording processes inside the film the read out of diffraction efficiency should be performed in transmission mode. In this case light wavelength (645 nm) that is not absorbed by film material should be used. Read out of *DE* in transmission mode was performed by laser L_2 (see Fig. 1a) at Bragg angle and photodiode PD_2. Recording and read out of *DE* was performed by 532 nm laser linearly polarized beams with $\pm 45^0$ configuration as described for Fig. 2 but simultaneously a read out of *DE* in transmission mode by 645 nm linearly polarized beam was done both with *s*-polarization direction (perpedicular to grating vector) and *p*-polarization direction (paralel to grating vector). The results of this experiment are represented in Fig. 5a, b. Fig.5a shows *DE* read out by 532 nm in reflection mode. It is seen that the formation process of SRG is not influenced by the polarization state of red (645 nm) read out laser beam. Quite different sight of *DE* curves has been observed for read out in transmission mode by *s*- and *p*-polarized 645 nm light (Fig. 5b). It is seen that the character of *DE* curves for *s*- and *p*-read out is different.

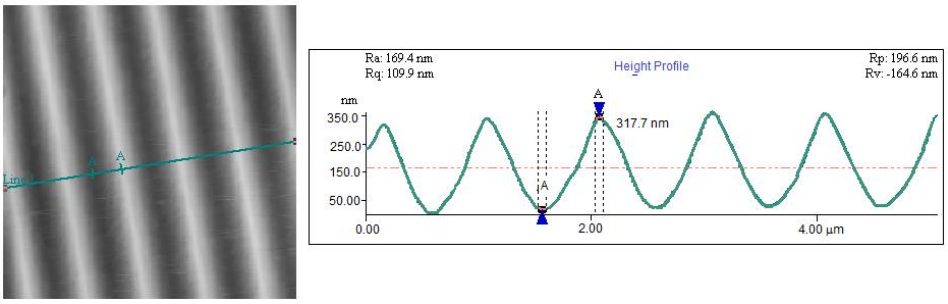

Fig.4 AFM pattern and SRG profile of $Ge_{25}Se_{75}$ film.

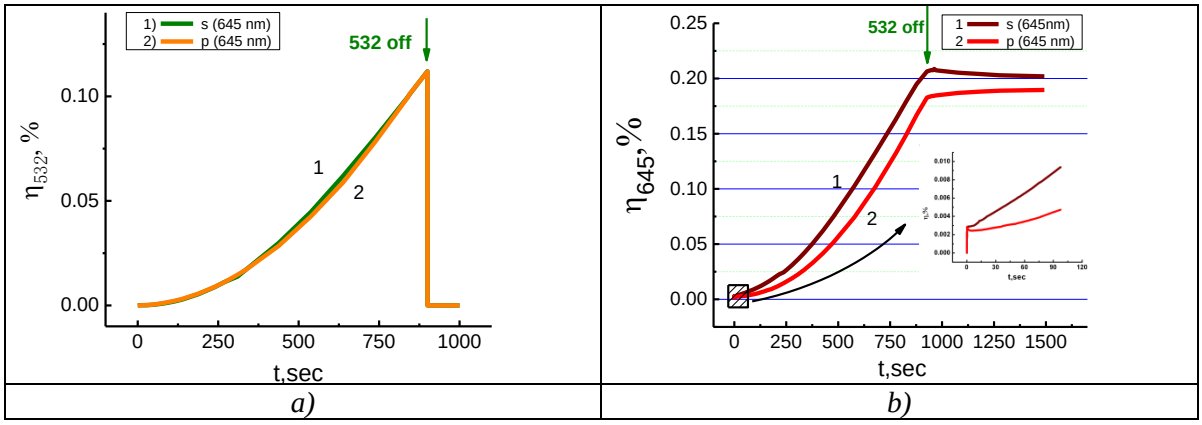

Fig. 5. Holographic recording in $Ge_{25}Se_{75}$ film by 532 nm laser beams with $+45^0$ and -45^0 polarization: a) readout of DE by 532 nm laser in reflection mode, b) readout of DE by 645 nm laser in transmission mode with s- and p-polarized beams. Intensity of recording beams $I_1=I_2=0.3$ W/cm^2, grating period 1 μm, intensity of 645 nm laser $I_0 = 420$ μW/cm^2. The inset shows initial stages of the DE curves.

The values of *DE* for *s*-read out are higher than for *p*-read out. In the first seconds of SRG recording a small but rapid increse of *DE* is established. Such increase is identical for both read out polarization states (see the inset of Fig. 5b). A continuous increase of *DE* for read out by *s*-polarization is observed in the further course of recording. For read out by *p*-polarized 645 nm laser beam a decrease of *DE* is observed in the first minute of recording. Afterwards an increase of *DE* takes place. The difference in *DE* values between these two read out states continues to increase during about 10 min and then it is stabilized. Relaxation of *DE* was observed when the recording laser (532 nm) was switched off. While *DE* of s-polarized readout beam in this process goes down, for *p*-polarized readout beam this parameter increases. After one day relaxation the values from the corresponding measurements are identical for both 645 nm laser polarization directions.

It is known that the largest SRG modulation can be obtained under $+45^0$:-45^0 (linearly orthogonal polarization with a direction 45^0 regarding the plane of recording scheme) and RCP:LCP (right and left circular polarization of beams) recording conditions [7,19,20]. It indicates that the existence of both light intensity and resultant electric field variations are essential to the formation of SRG on amorphous chalcogenide films. For both these configurations of recording beams there are components of resultant electric vector of light in interference pattern [21] that are parallel and perpendicular to the grating vector direction (Fig. 6a, b, c, d). The *DE* value is determined by phase shift within one grating period. If optical path *nd* (*d*, thickness and *n*, refractive index of the film) in material illuminated by *s* and *p* polarized light differs, grating is formed and *DE* appears. When the recording process is started, the photoinduced isomerisation and molecule alignment process takes place, and as a result photoinduced birefringence appears for red readout light $\{n(\|) \neq n(+)\}$ and volume polarization grating is formed. It is known that the amorphous chalcogenide films possess *negative* photoinduced birefringence, i.e. $n(\|)-n(+)<0$ [22, 23]. Before SRG formation, the *DE* both for *s* and *p* reading beams is equal (see inset in Fig. 5b and polarization direction distribution of recording and readout light in Fig. 6a and b). When SRG formation is started, a difference in *DE* values appears between readout with *s* and *p* polarized light (Fig. 6c and d). The course of *DE* curves for *s*- and *p*-polarized 645 nm light can be explained if we assume that the photoinduced displacement of the film material takes place from *s*- to *p*-polarized 532 nm light states in the film. In such case the volume polarization grating and SRG are in the phase using the *s*-polarized readout light and in antiphase for *p*-polarized readout. For *s*-readout a continuous increase of *DE* is established.The initial decrease of *DE* for *p*-readout can be explained by relief formation that reduces light phase difference between *s*- and *p* states (see Fig. 6d). The increase of difference between *s*- and *p*-readout shows that the photoinduced birefringence increases in the course of holographic recording.

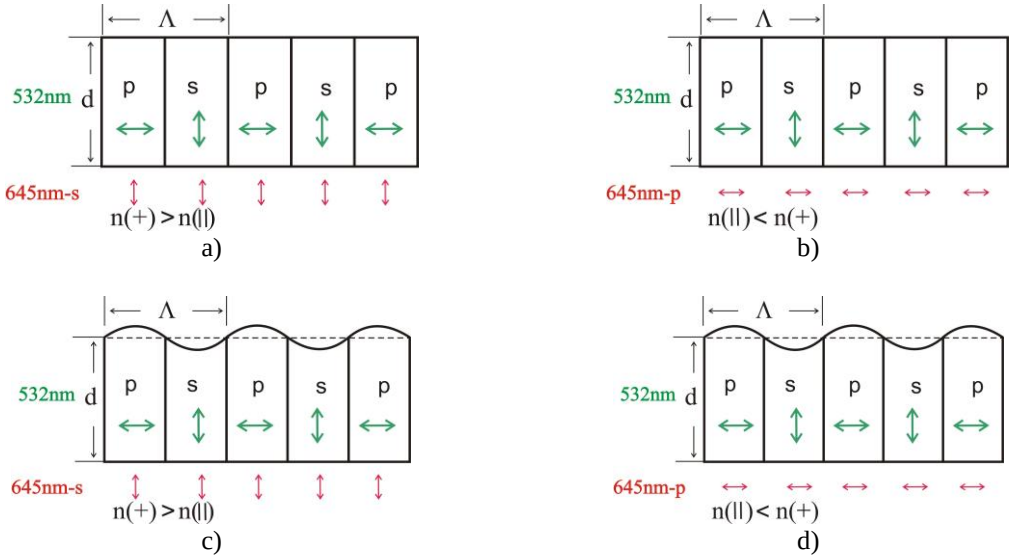

Fig. 6. s- and p-polarized light components in space-varying polarization pattern (green arrows) on sample for $+45^0$:-45^0 or LCP:RCP holographic recording with 532 nm laser and polarization direction of readout laser light 645 nm (red arrows). n(||) and n(+) – *refractive index of Ge-Se sample for 645 nm parallel and perpendicular to excitation light (532 nm) polarization direction on sample, respectively.*

As it is shown above (Fig. 5b and Fig. 6), the volume polarization grating and SRG are in the phase using the *s*-polarized readout light and in antiphase for *p*-polarized readout by 645 nm light. It means that *DE* readout values for *s*- and *p*-polarization states can be expressed as $\eta_s = \eta_r + \eta_v$ and $\eta_p = \eta_r - \eta_v$, respectively, where η_r is a *DE* due to SRG formation, but polarization component η_v is a *DE* as a result of photoinduced birefringence in film material. The value of η_v can be obtained from η_s and η_p measurements fom Fig. 5 b as $\eta_v = (\eta_s - \eta_p)/2$. The value of photoinduced birefringence (Δn) can be evaluated according to well known formula by Kogelnik for diffraction efficiency of phase holograms [24]:

$$\eta_v = \sin^2(\pi \, \Delta n \, d/\lambda \cos\varphi) \qquad (2)$$

where: readout laser wavelength λ=0.645 μm, d - film thickness and φ - Bragg angle of readout laser for 1 μm grating period. The value of Δn=5.3 10^{-3} was obtained at exposure dose about 0.6 kJ/cm^2.

The phase relationship between the exciting light field and the resulting surface deformation is crucial in understanding the mechanism of SRG formation. In order to estimate the influence of polarization state of the recording beams on surface relief formation direction and efficiency, we performed experiments with an illumination of amorphous $Ge_{25}Se_{75}$ film through optical slit. This experimental method is described in [16].

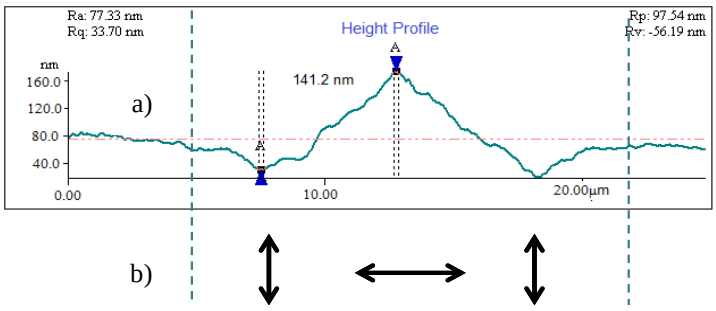

Fig. 7. The relationship between the resulting surface deformation (a) and the exciting light polarisation direction modulation (b) in amorphous $Ge_{25}Se_{75}$

After illumination the surface relief of the samples was studied by AFM. The obtained results illustrated in Fig. 7 show that photoinduced displacement of film material takes place from *s*- to *p*-polarization direction state in interference pattern of light. This result confirms the previous assumption based on *DE* measurements in transmission mode by *s*- and *p*- polarized 645 nm beams (Fig. 5b).

Fig. 8 shows the course of development of photoinduced birefringence in $GeSe_2$, Ge_2Se_8 and Se films measured by the method described in [17]. Experimental setup for these mesurements is shown in Fig. 2b. It is seen that photoinduced birefringence increases in the selenium rich films and simultaneously a reduction of induction period to attain the saturated state of Δn can be observed.

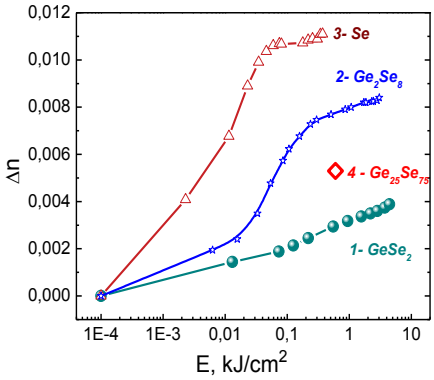

Fig. 8. Kinetics of photoinduced birefringence in Ge-Se films. Excitation and probing with 532 nm laser (curves 1, 2) and with 635 nm laser (curve 3) light illumination. Excitation light intensity $I \approx 0.3 W/cm^2$. Point (4) shows the $\Delta n = 5.3\ 10^{-3}$ for $Ge_{25}Se_{75}$ film obtained from holographic recording DE measurements described above.

Energy Dispersive Spectroscopy method was used to analyze compositional changes in the film after holographic recording of SRG with a period of 10 µm. Measurements were taken on virgin areas of the sample, together on high and low parts of the SRG as well.

Table 1. Results of EDS measurements taken of surface relief gratings

Virgin Film	Top of SRG	Bottom of SRG
$Ge_{19.1}\,Se_{80.9}$	$Ge_{18.7}\,Se_{81.3}$	$Ge_{19.6}\,Se_{80.4}$
$Ge_{24.2}\,Se_{75.8}$	$Ge_{23.7}\,Se_{76.3}$	$Ge_{24.7}\,Se_{75.3}$
$Ge_{29.1}\,Se_{70.9}$	$Ge_{28.6}\,Se_{71.4}$	$Ge_{29.5}\,Se_{70.5}$

Multiple measurements were taken in each of these areas and the results were averaged to determine how the composition is changed. The obtained results are summarized in Table 1.

It is seen that the process of SRG formation is accompanied by compositional changes in SRG *top* and *bottom* positions. The Se content increase in *top* and a decrease in *bottom* states on a grating has been observed. The changes of Ge content are in the opposite direction. The composition of the relief pattern varies by about 1% between high and low parts of surface grating, which confirms the role of mass transport in grating creation. Similar results were obtained in $As_{40}S_{15}Se_{45}$ films [25], where also an increase of Se content was observed in *top* places of grating after holographic recording. The obtained EDS measurements are in a good correlation with Raman spectroscopic investigations of SRG in selenium rich Ge_xSe_{100-x} films showing an importance of Se atoms in holographic grating formation process [15, 26]. An increase of twofold coordinated Se atom concentation in the films is accopanied by significant structural changes – a transition from rigid state ($x \geq 33.3$) to flexible (floppy) state for $x < 33.3$. In Se rich films ($x < 33.3$) a significant reduction of mean atomic bonding energy, glass transition temperature and optical bandgap has been found [18]. An excess of twofold coordinated selenium atoms cause an increase of atomic mobility and polarizability, thus promoting the photoinduced processes (photoinduced birefringence and mass displacement). It is known that linearly polarized light causes reorietation and arrangement of electric field sensitive structural units. These orientated structural units could be displaced by the gradient force of the electric field induced by polarized light components in interference pattern [21,27].

4. Conclusions

The photoinduced surface relief grating formation in chalcogenide Ge_xSe_{1-x} ($0 \leq x < 0.4$) thin films was studied in dependence on holographic recording laser wavelenght (491 nm, 532 nm, 561 nm and 594 nm). An increase of SRG formation efficiency and photoinduced birefringence was observed for the films with an excess of selenium content ($x < 0.33$). In the process of SRG formation the photoinduced displacement of film material takes place from *s*- to *p*-polarization direction position in interference pattern of light. EDS measurements showed a compositional changes between SRG *top* and *bottom* positions.

Our results suggest that a presence of an excess of twofold coordinated selenium atoms in the films causes an increase of atomic mobility and polarizability thus promoting the photoinduced processes (photoinduced birefringence and mass displacement). The linearly polarized light components in illumination pattern causes reorietation and arrangement of electric field sensitive structural units (dipoles). These orientated structural units could be displaced by the gradient force of an inhomogeneous electric field created by linearly polarized light components in interference pattern.

Acknowledgements

M. Reinfelde and J. Teteris highly appreciate the financial support by National research program IMIS2.

References

[1] H. Chomat, D. Ležal, I. Gregora, I. Srb, J. Non-Cryst. Solids **20**, 427 (1976).
[2] P. Rochon, E. Batalla, A. Natansohn, Appl. Phys. Lett. **66**, 136 (1995).
[3] D. Y. Kim, L. Li, S. K. Tripathy, J. Kumar, Appl. Phys. Lett. **66**, 1166 (1995).
[4] H. Hisakuni, K. Tanaka, Appl. Phys. Lett. **65**, 2925 (1994).
[5] S. Kokenyesi, I. Ivan, V. Takats, J. Palinkas, S. Biri, I.A. Szabo, J. Non-Cryst. Solids **353**, 1470 (2000).
[6] E. Potanina, J. Teteris, Chalcogenide Letters **10**, 449 (2013).

[7] K.E. Asatryan, T. Galstian, R. Vallee, Phys. Rev. Lett. **94**, 087401 (2005).
[8] F.S. De Vicente, M. Siu Li, Y. Messaddeq, J. Non-Cryst. Solids **348**, 245 (2004).
[9] K. Pavani, I. Naydenova, S. Martin, V. Toal, J. Opt. A: Pure Appl. Opt. **9**, 43 (2007).
[10] H. Audorff, R. Walker, L. Kador, H.W. Schmidt, Proc..SPIE **7233**, 723300 (2009).
[11] V.M. Kryshenik, M.L. Trunov, V.P. Ivanitsky, J. Optoelectron. Adv. Mater. **9**, 1949 (2007).
[12] K.H. Nam, J.H. Kim, H.B. Chung, Jap. Journ. Appl. Phys. **51**, 09MF04 (2012).
[13] M.R. Latif, I. Csarnovics, S. Kokenyesi, A. Csik, M. Mitkova, Can. J. Phys. **92**, 623 (2014).
[14] I. Csarnovics, C. Cserhati, S. Kokenyesi, M.R. Latif, M. Mitkova, P. Nemec, P. Hawlova, T. Nichol, M. Veres, J. Optoelectron. Adv. Mater. **18,** 793 (2016).
[15] I. Csarnovics, M. Veres, P. Nemec, M.R. Latif, P. Hawlova, S. Molnar, S. Kokenyesi, J. Non-Cryst. Solids **459,** 51 (2017).
[16] J. Teteris, U. Gertners, M. Reinfelde, Phys. St. Sol. **C 8** 2780 (2011).
[17] K. Klismeta, J. Teteris, IOP CS MSE, **77,** 012019 (2015).
[18] G. Yang, Y. Gueguen, J.C.Sangleboeuf, T. Rouxel, C. Boussard-Pledel, J. Troles, P. Lucas, B. Bureau, J. Non-Cryst.Solids **377**, 54 (2013).
[19] U. Gertners, J. Teteris, Opt. Mat. **32**, 807 (2010).
[20] U. Gertners, J. Teteris, J. Optoelectron. Adv. Mater. **11**, 1963 (2009).
[21] J. Teteris, M. Reinfelde, J. Aleksejeva, U. Gertners, Physics Procedia **44**, 151 (2013).
[22] V.G.Zhdanov, V.K.Malinovsky, Sov. Tech. Phys. Lett. **3**, 387 (1977).
[23] V. Boev, M. Mitkova, L.Nikolova, T.Todorov, P.Sharlandjiev, Opt. Mater. **13**, 389 (2000).
[24] H. Kogelnik, Bell Syst. Tech. J. **48**, 2909 (1969).
[25] M. Reinfelde, J. Teteris, J. Optoelectron. Adv. Mat. **13**, 1531 (2011).
[26] I.Csarnovics, M.R. Latif, T. Nichol, W. Kuang, M. Mitkova, M. Veres, J. Mater. Sci. Eng. A **5**, 78 (2015).
[27] V. Takats, M.I. Trunov, K. Vad, J. Hakl, D.I. Beke, Y. Kaganovskii, S. Kokenyesi, Mater. Lett. **160**, 558 (2015).